Subsurface thermal effects of land use changes

Daniela Nitoiu and Hugo Beltrami

Environmental Sciences Research Centre, St. Francis Xavier University, Antigonish, Nova Scotia, Canada

Received 16 March 2004; revised 12 October 2004; accepted 8 December 2004; published 2 February 2005.

[1] The International Heat Flow Commission global geothermal data set contains over 10,000 borehole temperature logs worldwide. Only about 10% of these data are currently used for climate studies because a number of known nonclimatic energy perturbations are superimposed on the climatic signal. Here we propose a first-order approach in terms of ground surface temperatures (GSTs) to attempt to correct borehole temperature data for the effects of one of these nonclimatic energy perturbations: deforestation. We simulate the ground surface temperature changes following deforestation using a combined power-exponential function describing the organic matter decay and recovery of the forest floor after a clear-cut. Application of this correction could allow many borehole data to be incorporated into the borehole climatology database and, at the same time, may allow land surface models to use geothermal data in regions of known land disruption in order to optimize land surface energy exchange parameterizations.

Citation: Nitoiu, D., and H. Beltrami (2005), Subsurface thermal effects of land use changes, *J. Geophys. Res.*, *110*, F01005, doi:10.1029/2004JF000151.

1. Introduction

[2] Solar energy is a fundamental factor determining climate. Almost half of that reaching the top of the atmosphere is absorbed by the terrestrial system [*Oke*, 1987; *Schneider*, 1990] and even an increase of 1% can influence the average global surface temperature by 0.5°–1°K [*Schneider*, 1995]. However, precisely determining such a small but important quantity of energy is difficult from meteorological data because of the uncertainties associated with the measurements of atmospheric variables [*Karl et al.*, 1989].

[3] In a forest ecosystem, only 5–20% of the short-wave solar radiation incident on the forest canopy reaches the land surface [*Oke*, 1987; *Beltrami*, 2001a]. Therefore any removal of trees results in a substantial increase in solar radiation reaching the land surface, a reduction of the leaf area involved in transpiration [*Aber*, 1995], and in general, a rearrangement of the energy budget at the air-ground interface [*Geiger et al.*, 1995].

[4] Feedback effects of large-scale deforestation are important and extend beyond the limits of the area undergoing land use change, influencing the global climate [*Bonan et al.*, 1992; *Pielke et al.*, 1998; *Chase et al.*, 2000]. *Hansen et al.* [1998] and *Betts* [2001] compared the radiative forcing caused by land use changes, by greenhouse gases, aerosols and stratospheric ozone, and found them to be of comparable magnitudes. There is also clear evidence that land use induced subsurface thermal changes alter biogeochemical feedbacks including the CO_2 exchange between land and the atmosphere, further influencing the climate [*Risk et al.*, 2002a, 2002b].

0148-0227/05/2004JF000151$09.00

[5] The organic matter layer covering the forest floor is an important thermal insulator [*Yoshikawa et al.*, 2003]. Its variability after deforestation has been described by *Covington* [1981] using a chronosequence study in northern hardwood forest stands. The study found a decrease of almost 50% of forest floor mass during the first 20 years after deforestation, followed by a slow recovery with a return to precutting levels after almost 100 years (see Figure 1). The rapid loss of the forest floor organic mass was initially explained by the increased moisture and soil temperature following clear-cutting that accelerated the rate of decomposition and by the decrease in the woody litter inputs [*Covington*, 1981]. The subsequent increase of forest floor organic matter mass is thought to be due to the increase in woody litter inputs after the forest regrowth. Although not all the processes governing Covington's curve are well understood or explained [*Federer*, 1984; *Johnson et al.*, 1985; *Yanai et al.*, 2003], several studies have made use of this function to address a variety of subjects. *Mattson and Smith* [1993] found that forest floor mass changes after deforestation in northern West Virginia obey Covington's model. *Houghton et al.* [1983, 1987] used this model to estimate the carbon loss through deforestation of temperate forest soils. *Hornbeck et al.* [1986] and *Yanai* [1992] applied Covington's model to estimate nutrient release and phosphorus accumulation in postharvest hardwood forest floors in New Hampshire. *Brais et al.* [1995] confirmed Covington's observations in northwestern Quebec. In tropical regions, *Lugo and Brown* [1986] estimated the effects of deforestation on soil carbon content using the chronosequence approach. Some studies [*Yanai et al.*, 2003] claim that discrepancies between recent observations and Covington's model may be due to the differences in physical disturbances of the sites caused by recent, more disruptive stand harvest methods [*Johnson et al.*, 1995].

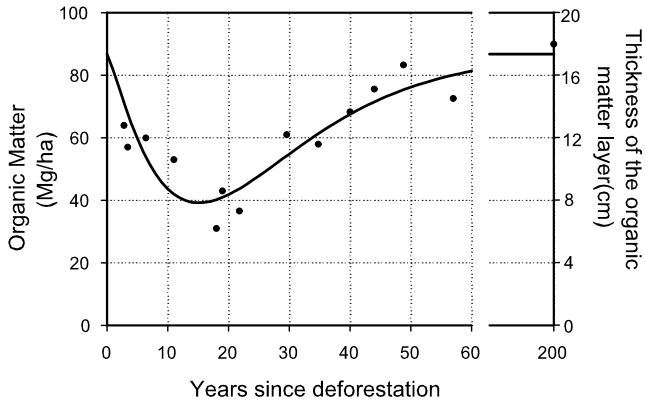

Figure 1. Forest floor organic matter mass as a function of time for the original chronosequence studied by *Covington* [1981]. The thickness of the organic matter layer was estimated for a density of 0.05 gm^{-3} [*Yoshikawa et al.*, 2003]. The initial amount of forest floor organic matter mass varies widely; it is dependent on the species and age of the stand. Modified from *Covington* [1981].

[6] Although many other feedbacks follow deforestation, a common and well accepted effect, according to models [*Dickinson and Henderson-Sellers*, 1988; *Shukla et al.*, 1990; *Dickinson and Kennedy*, 1992; *Zhang et al.*, 1996; *Betts*, 2001; *Arribas et al.*, 2003], and measurements [*Edwards and Ross-Todd*, 1983; *Londo et al.*, 1999], is the increase of surface temperature in tropical and temperate areas.

[7] In the context of the energy balance at the air-ground interface and the thermal regime of the subsurface, systematic variations of the thickness of the organic matter, acting as a thermal insulation layer covering the forest floor [*Fleming et al.*, 1998; *Bhatti et al.*, 2000; *Yoshikawa et al.*, 2003], affect the energy balance at the ground surface in a similar fashion as a time varying snow cover does in winter at high latitudes [*Beltrami and Kellman*, 2003].

[8] While the organic matter layer decreases after a clear-cut or a forest fire and the albedo decreases [*Yoshikawa et al.*, 2003], the evapotranspiration decreases and more energy is absorbed into the subsurface increasing the ground surface temperature, accounting for the soil temperature differences between forests and cleared areas. Measured ground surface temperature differences between the forest and open areas in Atlantic Canada are between 2° and 3°K [*Beltrami*, 2001a; *Beltrami and Kellman*, 2003]. Comparable values were found by *de Souza et al.* [1996], who measured the soil temperature beneath forest and pasture in eastern Amazonia and in other regions [*Guldin and Barnett*, 2004; *Kraske*, 1992; *Lytle and Cronan*, 1998; *Plotnikoff et al.*, 2002].

[9] As the forest recovers, the organic matter layer thickness increases and the ground surface temperature approaches precut values. The transient thermal signal caused by the rearrangement of the energy balance at the air-ground interface and by the variations of the thickness of the forest floor organic matter layer are recorded in the underground superimposed on the climatic signature and the steady state geothermal field.

[10] Processes such as deforestation modify the surface energy balance and change the boundary conditions of the climate system [*Zeng and Neelin*, 1999]. The ground surface is the lower boundary for almost 30% of the atmosphere, and the ground/atmosphere interaction involves exchanges of heat, moisture and momentum. It is thus important to have a robust parameterization of the energy balance at the surface of the Earth. Precise information may then be obtained from borehole temperature data since the ground is very sensitive to small energy changes at its surface and continuously records these imbalances [*Lachenbruch and Marshall*, 1986]. While the amplitude of daily variations of the surface heat flux are much higher than the changes caused by events such as deforestation or snow cover variations, over the long-term, small energy imbalances become important, and since the ground acts as a high-frequency filter of energy fluctuations [*Vasseur et al.*, 1983; *Beltrami et al.*, 2000; *Baker and Baker*, 2002], it records these long-term trends as temperature perturbations superimposed on the equilibrium state. Energy imbalances at the ground surface as small as 17 m Wm^{-2}, persistent over 200 years, can be easily detected from borehole temperature data [*Beltrami et al.*, 2000]. Since *Lane* [1923] recognized that the energy imbalances at the surface of the Earth are propagated and recorded into the ground, much work has been done to reconstruct the ground surface temperature history (GSTH) [*Beltrami and Harris*, 2001, and references therein; *Beltrami et al.*, 2003] and the energy balance at the Earth's surface [*Beltrami et al.*, 2000; *Beltrami*, 2002] from borehole temperature data.

[11] It has long been known that alterations of the surface conditions (i.e., deforestation, snow cover variations) can have a significant effect on the subsurface thermal regime [*Lewis and Wang*, 1998; *Geiger et al.*, 1995]. Indeed, many borehole temperature-depth data from around the world have been excluded from the global data set dedicated to borehole climatology because they are located in areas subjected to land use changes including deforestation [*Guillou-Frottier et al.*, 1998]. For areas where the deforestation can be dated, we propose to use a first-order approach, presented here, to correct borehole temperature data by removing the nonclimatic temperature perturbations from the measured temperature-depth profiles. This would allow a significant enlargement of the present data set. We demonstrate that correcting these "contaminated" data may be possible if the time and the character of the land use change is known. The application of the correction method to one temperature-depth profile from central Canada affected by deforestation, shows that the effects of the disturbance are removed and the GSTH obtained represents the actual climate signal: a ground surface warming that is in good agreement with the warming trends revealed by other studies in the same region.

2. Theory

[12] Reconstruction of ground surface temperature histories from geothermal data assumes that the thermal regime of the ground is dominated by conduction and that there is no lateral propagation of the heat; thus surface temperature

variations propagate into the subsurface following the one-dimensional time-dependent heat conduction equation [*Carslaw and Jaeger*, 1959]

$$\frac{\partial T}{\partial t} = \kappa \frac{\partial^2 T}{\partial z^2}, \tag{1}$$

where $\kappa(z)$ is the thermal diffusivity, z is the depth, and T is the temperature.

[13] When the subsurface temperatures are not disturbed by nonclimatic factors like topography, ground water flow or variations in thermal properties, the temperature at depth z is given, at any time, by the quasi steady state surface temperature T_0, and the temperature perturbation $T_t(z)$ caused by the time varying ground surface temperature according to

$$T(z) = T_0 + q_0 R(z) + T_t(z), \tag{2}$$

where q_0 is the quasi steady state surface heat flow density and $R(z)$ is the thermal depth:

$$R(z) = \sum_{i=1}^{N} \frac{\Delta z_i}{\lambda_i}, \tag{3}$$

where λ_i is the thermal conductivity over the depth interval Δz_i.

[14] If the past variations of ground surface temperature are modeled as a series of K step changes in temperature, then the subsurface temperature signatures from each step change are superimposed and the temperature perturbation at depth z is given by [*Mareschal and Beltrami*, 1992]

$$T_t(z) = \sum_{k=1}^{K} T_k \left[\mathrm{erfc}\left(\frac{z}{2\sqrt{\kappa t_k}}\right) - \mathrm{erfc}\left(\frac{z}{2\sqrt{\kappa t_{k-1}}}\right)\right], \tag{4}$$

where T_k is the ground surface temperature, each value representing an average over a time ($t_k - t_k{-}_1$), and erfc is the complementary error function.

[15] The inverse problem determines T_0, q_0 and the ground surface temperature history (GSTH), represented through $T_1,\ldots,T_k$, from $T(z)$. Alternatively, T_0 and q_0 can be estimated independently from the upward continuation from the deepest part of the profile, least affected by recent ground surface temperature changes.

[16] The solution for $T_t(z)$ requires equation (2) to be evaluated at every depth where data exist, forming a system of linear equations with $k + 2$ unknowns which can be written as

$$\Theta_j = A_{ji} X_i, \tag{5}$$

where Θ_j is a column vector containing the j values of temperature ($\Theta_1,\ldots, \Theta_j$) measured at depth z_j, X_i is a column vector containing the $i + 2$ unknown model parameters (T_0, q_0, $T_1,\ldots, T_k$); A_{ji} is a ($j \times i$) matrix which contains 1 in the first column, the thermal resistance at depth z_j, $R(z_j)$, in the second column, and the differences between complementary error functions at times t_{k-1} and t_k for depth z_j in columns 3 to $k + 2$:

$$\begin{pmatrix} \Theta_1 \\ \Theta_2 \\ \vdots \\ \Theta_j \end{pmatrix} = \begin{pmatrix} 1 & R_1 & A_{1,3} & A_{1,4} & \ldots & A_{1,k+2} \\ 1 & R_2 & A_{2,3} & A_{2,4} & \ldots & A_{2,k+2} \\ \vdots & \vdots & \vdots & \vdots & \ddots & \vdots \\ 1 & R_j & A_{j,3} & A_{j,4} & \ldots & A_{j,k+2} \end{pmatrix} \begin{pmatrix} T_0 \\ q_0 \\ T_1 \\ \vdots \\ T_k \end{pmatrix} \tag{6}$$

$$A_{j,k+2} = \mathrm{erfc}\left(\frac{z_j}{2\sqrt{\kappa t_k}}\right) - \mathrm{erfc}\left(\frac{z_j}{2\sqrt{\kappa t_{k-1}}}\right). \tag{7}$$

[17] The system of linear equations (5) can be solved for a GSTH, using Singular Value Decomposition (SVD) [*Lanczos*, 1961; *Jackson*, 1972; *Menke*, 1989]. Any matrix $A(j \times i)$ can be decomposed as $A = U\Lambda V^T$, where Λ is a $j \times i$ diagonal matrix which contains on the diagonal entries the nonzero singular values $\lambda_{(r)}$ of matrix A, $r = 1,\ldots, R$, R is the rank of A; $\lambda_{(r)}$ are the square roots of the eigenvalues of the symmetric matrix $A^T A$. U is a $j \times j$ column orthogonal matrix, each column forming a vector, and all j normed vectors (u_j) forming an orthonormal basis spanning the data space (i.e., they are dependent and are generated solely from data). V is an $i \times i$ orthogonal matrix, each column forming a vector, and all i normed vectors (v_i) forming an orthonormal basis spanning the model space (i.e., they are dependent on model geometry and physics of heat diffusion). Also, the rows of matrix V are i normed vectors forming an orthonormal basis. The column vectors v_i are also eigenvectors corresponding to the eigenvalues of $A^T A$. The normed eigenvectors that span the model space, v_i, could be interpreted as the effect on the subsurface of a GSTH given by the normed eigenvectors that span the data space, u_j [*Vasseur et al.*, 1983]. A general solution is given by *Lanczos* [1961]:

$$X = V\Lambda^{-1} U^T \Theta. \tag{8}$$

The unknowns given by the generalized solution (7) can be written explicitly as

$$X_i = \Theta_j \left(\frac{v_{ir} u_{rj}}{\lambda_{(r)}}\right). \tag{9}$$

[18] Since the variance of the estimated model parameters can be written as

$$\sigma_i^2 = \sum_{r=1}^{R} \frac{v_{ri}^2}{\lambda_{(r)}^2}, \tag{10}$$

it can be seen that any error in the data will be multiplied by $1/\lambda_{(r)}$ and will be amplified for the very small singular values. The square root of the ratio of the largest to the smallest eigenvalue measures the amplification of the noise in the direction of the smallest eigenvalue. So, it is necessary to eliminate the singular values which are smaller than a cut-off value. The solution consists of linear combinations of model parameters corresponding only to

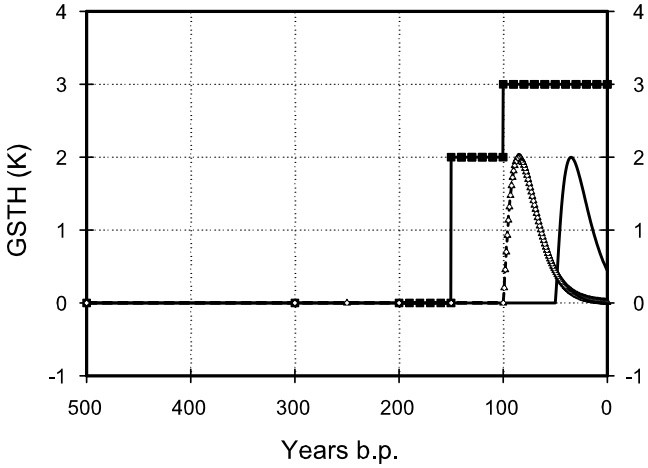

Figure 2. Synthetic ground surface temperature history (GSTH) (squares) and the ground surface temperature (GST) model variations due to deforestation events taking place 100 years before present (ybp) (triangles) and 50 ybp (line).

the highest eigenvalues, and thus it differs from the "true" solution but it has a small variance. However, for noise free data or with a low noise level, the resolution can be improved by including more singular values in the inversion [*Beltrami and Mareschal*, 1995], that is, reconstructing the GSTH with a larger number of principal components.

3. Analysis

[19] Since the energy balance at the forest floor and thus the ground surface temperature are affected by the removal of vegetation and by the variations of the thickness of the forest floor organic matter layer [*Yoshikawa et al.*, 2003], we propose a model based on Covington's curve to describe the pattern of the ground surface temperature (GST) variation after deforestation:

$$T_g = At^B e^{Ct^D} + T_0, \tag{11}$$

where T_g represents the GST, t is the time in years since deforestation, and $A = 5.25$, $B = 1.24$, $C = -0.0649$, $D = 1.063$, and T_0, are regression coefficients [*Covington*, 1981].

[20] We assume that in the first years after deforestation, when the surface is covered by debris and small-size sparse vegetation, the shape of the GST variation is governed by the function At^B, with A and B positive values, and the temperature increases to a maximum of 2°K [*de Souza et al.*, 1996; *Beltrami*, 2001a; *Beltrami and Kellman*, 2003; *Yoshikawa et al.*, 2003]. As the forest floor organic matter recovers, we assume that the temperature decreases to its original value, T_0.

3.1. Synthetic Example

[21] In order to illustrate the procedure we generated a synthetic, base GSTH consisting of two temperature step increases, of 2°K and of 1°K, occurring at 150 and 100 years before present (ybp) respectively. To examine how the time of deforestation affects the ground surface and subsurface temperatures, we assumed two cases of deforestation: in the first case the deforestation event occurred 100 ybp and, in the second case, 50 ybp. Following equation (10), deforestation-induced GST variations were generated for both cases. These and the base GSTH are shown in Figure 2. Figure 3 shows the subsurface temperature perturbation profiles, from the surface to 500 m, at 10 m intervals, generated as a forward problem from the deforestation models shown in Figure 2. The shallowest 20 m reflect the annual variation of the ground surface temperature and were eliminated to simulate typical borehole temperature data. We assumed constant thermal conductivity ($\lambda = 3.0$ Wm^{-1} K^{-1}) and thermal diffusivity ($\kappa = 10^{-6}$ m^2 s^{-1}) [*Cermak and Rybach*, 1982]. The deforestation event that took place 50 ybp caused a subsurface thermal signal that was propagated to almost 150 m with a maximum perturbation of the upper part of the profile. The subsurface temperature perturbations caused by the deforestation that occurred 100 ybp were propagated deeper into the ground (i.e., almost 200 m) but with a maximum disturbance of the profile at 60 m. The amplitude of the perturbations caused by older deforestation events were smoothed out by the diffusion process. Subtracting the nonclimatic temperature perturbations from the base temperature-depth profile completes the correction. The uncorrected and the corrected profile for both modeled cases of deforestation are shown in Figure 4.

[22] In order to assess qualitatively and quantitatively the effects of the correction on the typical GSTH recovered by inversion, we inverted the profiles shown in Figure 4 using a model consisting of a series of 25 surface temperature changes, each representing a temperature averaged over 20 years [*Mareschal and Beltrami*, 1992]. The GSTHs

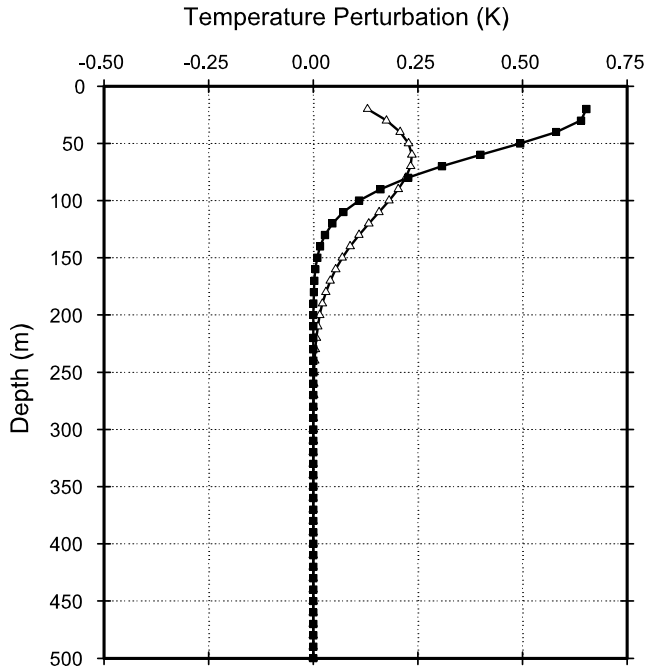

Figure 3. Subsurface temperature perturbation profiles generated from the GST model variations, as a forward solution, due to deforestation taking place 100 ybp (triangles) and 50 ybp (squares).

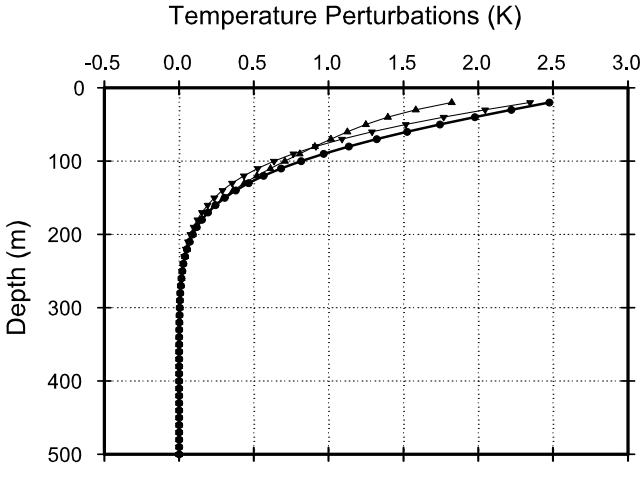

Figure 4. Temperature perturbation profiles generated from the base GSTH: the base (uncorrected) profile (circles), corrected for deforestation at 100 ybp (inverted triangles), and corrected for deforestation at 50 ybp (triangles).

recovered from inversion are shown in Figure 5. The inversion of the corrected temperature perturbations profiles shows that the effects of deforestation were removed for both models and that the greatest perturbation of the GST was caused by the more recent deforestation event, at 50 ybp.

[23] A clear-cut event taking place 100 years ago which is followed by a total recovery of the initial forest, will have a subsurface signature increasing the ground temperatures as a function of depth. However, if at the time of the observation, the forest recovery is complete and the GST has reached the precutting value, the differences between the synthetic and the corrected GSTHs (Figure 5) for the most recent 20 years, are almost nonexistent. For the second case, when the deforestation event takes place in more recent times (i.e., 50 ybp), the corrected GSTH shows the removal of the 2°K difference between forested and open areas, and since the forest is still recovering, the GST does not reach the precutting value, as it does for the 100 ybp event model.

3.2. Application to Field Data

[24] Many borehole temperature data have been excluded from studies of recent climate changes because of different anthropogenic influences such as deforestation and forest fires. *Guillou-Frottier et al.* [1998] rejected data from the Pipe Mine site, central Canada, because of the great warming indicated by these profiles, more than 3°K, attributed to land clearing. *Gosselin and Mareschal* [2003] suggested that the great warming recorded at the Pipe Mine site after 1960 might be caused by deforestation.

[25] To illustrate the correction method on real borehole temperature data, one temperature profile from central Canada was analyzed: The Pipe Mine 9411 log is located 55°29′10″N, 98°07′54″W, 32 km southwest of Thompson, Manitoba. The borehole site was deforested around 1960 when a highway and power line were built and when the first mine in Thompson opened in 1961 [*Gosselin and Mareschal*, 2003]. In 1994 when the temperature-depth profile was measured the site was covered by vegetation.

[26] We applied the correction to these data in the same fashion as for the synthetic data shown above, by subtracting the subsurface temperature perturbations caused by the deforestation event 34 ybp from the measured temperature-depth profile. The uncorrected and the corrected profiles are shown in Figure 6. The reconstruction of the GSTHs, from both corrected and uncorrected profiles, was performed for a series of 50 step temperature changes, each representing an average surface temperature over 20 years. The results for the last 500 years are shown in Figure 7. The inversion of the uncorrected profile reveals a GST increase of almost 1.5°K in the recent 40 years when the deforestation event took place, superimposed on a long-term increase that started around 200 ybp. After correction, the GSTH at the Pipe Mine 9411 site shows a warming of 1.7°K over the last two centuries which is good agreement with the

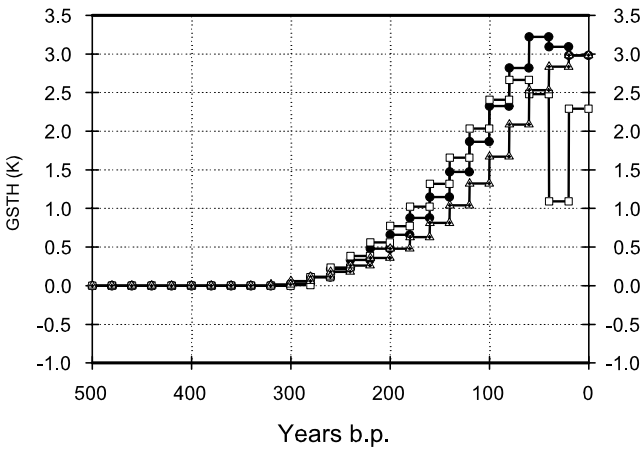

Figure 5. Ground surface temperature histories recovered from inversion of the uncorrected (circles), corrected for deforestation 100 ybp (triangles), and corrected for deforestation 50 ybp (squares) temperature perturbation profiles.

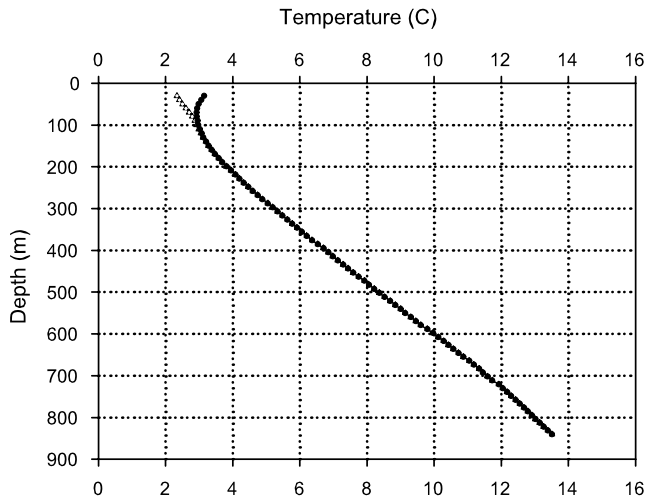

Figure 6. Application of the correction method described in text to one borehole from central Canada: the measured temperature profile (circles) and the corrected temperature profile for a deforestation event that took place 34 ybp (triangles).

warming trends found in the region [*Beltrami et al.*, 1992; *Guillou-Frottier et al.*, 1998; *Gosselin and Mareschal*, 2003].

4. Discussion and Conclusions

[27] Vegetation is an important factor affecting the surface temperature. Recent studies [*Kaufmann et al.*, 2003] showed that the increased vegetation cover during the summer time in North America and Eurasia, have slowed down the temperature increase during the last 20 years. Clearing by deforestation or by forest fire increases the energy reaching the land surface. The increase in albedo is compensated by the decrease in evapotranspiration, and the net energy transfer into the ground increases the surface temperature in the first years after land clearing [*Dickinson and Henderson-Sellers*, 1988; *Shukla et al.*, 1990; *Dickinson and Kennedy*, 1992; *Zhang et al.*, 1996]. As a new forest grows, the ground surface temperature decreases to near its original value.

[28] In the method described here we assumed that after deforestation the forest regrows to the preharvest state. Given that the time necessary for the GST (and organic matter layer) to return to the undisturbed value is almost 100 years [*Covington*, 1981], it is clear that the subsurface temperature perturbations due to a more recent clear-cut event (50 ybp) are still important. Although the shapes of the GST variation for both deforestation models (Figure 2) are quite similar, the effects on the subsurface temperatures (Figures 3 and 4) are larger for the more recent event. Subsurface disturbances caused by older deforestation events propagate to larger depths, but much of their magnitude has decayed because of the character of the heat diffusion in the subsurface. This behavior is accentuated for a model consisting of a rapid GST increase followed by a slower decrease to the preharvest value, because the applied disturbance is present only for a limited time and the subsurface temperature perturbations dissipate with time.

[29] There are several situations that can be incorporated into this first-order model. Complete forest regeneration to a preharvest state (Figure 8, line 4) is not common and in most cases the new growth forest will be different in density and species. Thus the GST will settle to a different value (perhaps higher) than the preharvest GST (Figure 8, line 3). The GST variation post clear-cut could be still described by this model, but with a new end-point GST corresponding to the new equilibrium state.

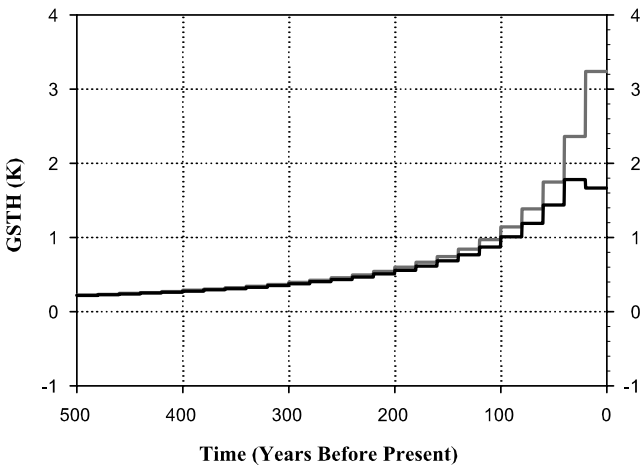

Figure 7. Ground surface temperature histories recovered from inversion from the uncorrected (shaded line) and the corrected (black line) temperature profiles.

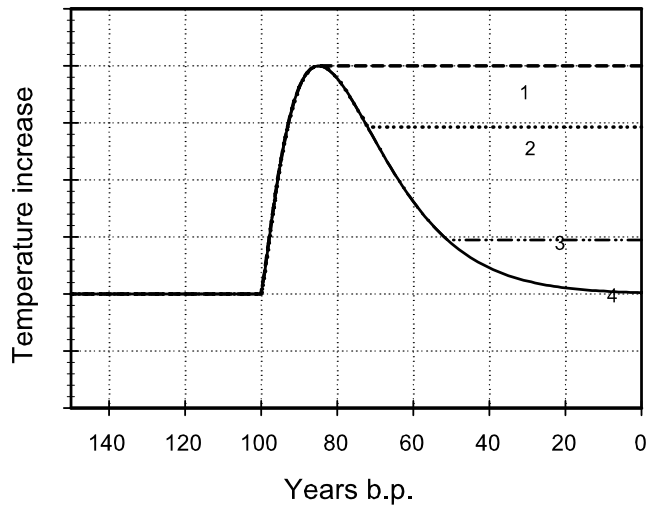

Figure 8. Generic model of ground surface temperature variations for different types of land covers as terminal point after deforestation: bare ground (line 1), grassland (line 2), different forest than the initial one (line 3), and return to the same state as before deforestation (line 4).

[30] If the forest is transformed into grassland, or bare ground, then the GST model might be described as lines 2 and 1 in Figure 8, respectively. However, in the case of a bare ground end point, the GST increase may be much higher than 2°K [*Geiger et al.*, 1995].

[31] The subsurface thermal effects due to a series of deforestation events could also be estimated with this model. A sequence of deforestation events is typical for today's forests lands in Canada, where maximization of yield calls for harvest at 50 year intervals [*McGrath*, 1999; *Erdle*, 1999]. Since the subsurface temperature perturbation caused by a deforestation event that occurred 50 ypb are quite large in the upper 100 m, borehole temperature data located in present-day forested areas that might have such a land cover history should be corrected for these effects.

[32] The practice of partial harvesting is more difficult to model, but is probably negligible as a correction for geothermal data since this practice is too recent, although this type of process may also be included in this method by decreasing the GST rate of change after deforestation. The adjustments in the correction model can be easily made once the type of regrowth is known. Work on modeling the effects of different harvesting practices is in progress.

[33] We have shown that subsurface temperatures are affected by disturbances (especially for events in the recent past) but these effects can be removed if the time when the disturbance occurred is known. The application of this correction method to the "contaminated" borehole temperature data from the global geothermal data set would allow inclusion of data from "contaminated" sites in the borehole climatology database and enhance the GSTH

reconstructions from geothermal data for the last millennium. A full energy balance, vegetation, and soil process model would be the desired method of correction of geothermal data, but the characterization of surface conditions at each of the 10,000 borehole sites for inclusion in a full model, seems unattainable at least in the near future.

[34] The results from this work may be useful for land surface models where the long-term energy storage in the subsurface has generally been neglected [*Baker and Baker*, 2002]. Furthermore, evaluation of the surface energy balance history from geothermal data could provide the boundary conditions needed for land surface and general circulation model improvements [*Beltrami et al.*, 2000; *Beltrami*, 2001b; *Baker and Baker*, 2002] and, perhaps more importantly, subsurface temperature data may provide a way to discriminate between rival land surface energy partition subroutines and optimize land surface energy exchange parameterizations.

[35] **Acknowledgments.** This research was funded by the Canadian Foundation for Climate and Atmospheric Sciences (CFCAS), the Natural Sciences and Engineering Research Council of Canada (NSERC), and the Atlantic Innovation Fund (AIF). We thank C. Gosselin for providing the information regarding the land cover history of the Pipe mine site. Amanda Diochon helped us digest the chronosequence work. Comments by A. Diochon, E. Bourlon, D. Risk, L. Kellman, the Associate Editor, and an anonymous reviewer helped us to improve this manuscript.

References

Aber, D. J. (1995), Terrestrial ecosystems, in *Climate System Modeling*, edited by K. E. Trenberth, pp. 173–200, Cambridge Univ. Press, New York.

Arribas, A., C. Gallardo, M. A. Gaertner, and M. Castro (2003), Sensitivity of the Iberian Peninsula climate to a land degradation, *Clim. Dyn.*, *20*, 477–489.

Baker, M. J., and D. G. Baker (2002), Long-term ground heat flux and heat storage at mid-latitude site, *Clim. Change*, *54*, 295–303.

Beltrami, H. (2001a), On the relationship between ground temperature histories and meteorological records: A report on the Pomquet station, *Global Planet. Change*, *29*, 327–349.

Beltrami, H. (2001b), Surface heat flux histories from inversion of geothermal data: Energy balance at the Earth's surface, *J. Geophys. Res.*, *106*, 21,979–21,993.

Beltrami, H. (2002), Climate from borehole data: Energy fluxes and temperatures since 1500, *Geophys. Res. Lett.*, *29*(23), 2111, doi:10.1029/2002GL015702.

Beltrami, H., and R. N. Harris (2001), Inference of climate change from geothermal data, *Global Planet. Change*, *29*, 148–352.

Beltrami, H., and L. Kellman (2003), An examination of short- and long-term air-ground temperature coupling, *Global Planet. Change*, *38*, 291–303.

Beltrami, H., and J.-C. Mareschal (1995), Resolution of ground temperature histories inverted from borehole temperature data, *Global Planet. Change*, *11*, 57–70.

Beltrami, H., A. M. Jessop, and J.-C. Mareschal (1992), Ground temperature histories in eastern and central Canada from geothermal measurements: Evidence of climatic change, *Global Planet. Change*, *98*, 167–184.

Beltrami, H., J. Wang, and R. L. Bras (2000), Energy balance at the Earth's surface: Heat flux history in eastern Canada, *Geophys. Res. Lett.*, *27*, 3385–3388.

Beltrami, H., C. Gosselin, and J.-C. Mareschal (2003), Ground surface temperatures in Canada: Spatial and temporal variability, *Geophys. Res. Lett.*, *30*(10), 1499, doi:10.1029/2003GL017144.

Betts, R. A. (2001), Biogeophysical impacts of land use on present-day climate: Near-surface temperature change and radiative forcing, *Atmos. Sci. Let.*, *1*, doi:10.1006/asle.2001.0023.

Bhatti, J. S., R. L. Fleming, N. W. Foster, F.-R. Meng, C. P. A. Bourque, and P. A. Arp (2000), Simulations of pre- and post-harvest soil temperature, soil moisture, and snowpack for Jack pine: Comparison with field observations, *For. Ecol. Manage.*, *138*, 413–426.

Bonan, G. B., D. Pollard, and S. L. Thompson (1992), Effects of boreal forest vegetation on global climate, *Nature*, *359*, 716–718.

Brais, S. C., C. Camire, and D. Pare (1995), Impacts of whole-tree harvesting and winter windrowing on soil-pH and base status of clayey sites of northwestern Quebec, *Can. J. For. Res.*, *25*, 997–1007.

Carslaw, H. S., and J. C. Jaeger (1959), *Conduction of Heat in Solids*, 2nd ed., 510 pp., Oxford Univ. Press, New York.

Cermak, V., and L. Rybach (1982), Thermal conductivity and specific heat of minerals and rocks, in *Landolt-Bornstein; Zahlenwerte und Funktionen aus Naturwissenschaften und Technik*, edited by G. Angenheister, pp. 305–343, Springer, New York.

Chase, T. N., R. A. Pielke, T. G. F. Kittel, R. R. Nemani, and S. W. Running (2000), Simulated impacts of historical land cover changes on global climate in northern winter, *Clim. Dyn.*, *16*, 93–105.

Covington, W. W. (1981), Changes in the forest floor organic matter and nutrient content following clear cutting in northern hardwoods, *Ecology*, *62*, 41–48.

de Souza, J. R. S., F. M. A. Pinheiro, R. L. C. de Araujo, H. S. Pinheiro Jr., and M. G. Hodnett (1996), Temperature and moisture profiles in soil beneath forest and pasture areas in eastern Amazonia, in *Amazonian Deforestation and Climate*, edited by J. H. C. Gash et al., pp. 125–139, John Wiley, Hoboken, N. J.

Dickinson, R. E., and S. Henderson-Sellers (1988), Modelling tropical deforestation: A study of GCM land surface parameterizations, *Q. J. R. Meteorol. Soc.*, *114*, 439–462.

Dickinson, R. E., and P. Kennedy (1992), Impacts on regional climate of Amazon deforestation, *Geophys. Res. Lett.*, *19*, 1947–1950.

Edwards, N. T., and B. M. Ross-Todd (1983), Soil carbon dynamics in a mixed deciduous forest following clear-cutting with and without residue removal, *Soil Sci. Soc. Am. J.*, *47*, 1014–1021.

Erdle, T. (1999), Forest level effects of pre-commercial and commercial thinnings, in *Thinning in the Maine Forest: Conference Proceedings, 15–16 November 1999*, edited by R. G. Wagner et al., pp. 19–28, Univ. of Maine, Augusta.

Federer, C. A. (1984), Organic matter and nitrogen content of the forest floor in even-aged northern hardwoods, *Can. J. For. Res.*, *14*, 763–767.

Fleming, R. L., T. A. Black, R. S. Adams, and R. J. Stathers (1998), Silvicultural treatments, microclimatic conditions and seedling response in southern interior clearcuts, *Can. J. Soil Sci.*, *78*, 115–126.

Geiger, R., R. H. Aron, and P. Todhunter (1995), *The Climate Near the Ground*, 5th ed., 528 pp., Vieweg, Braunschweig, Germany.

Gosselin, C., and J.-C. Mareschal (2003), Variations in ground surface temperture histories in the Thompson Belt, Manitoba, Canada: Environment and climate changes, *Global Planet. Change*, *39*, 271–284.

Guillou-Frottier, L., J.-C. Mareschal, and J. Musset (1998), Ground surface temperature history in central Canada inferrred from 10 selected borehole temperature profiles, *J. Geophys. Res.*, *103*, 7385–7397.

Guldin, J. M., and J. P. Barnett (2004), Microclimatic conditions after reproduction cutting in shortleaf pine stands in the Ouachita Mountains, in *Proceedings of the 12th Biennial Southern Silvicultural Research Conference, Gen. Tech. Rep. SRS-71*, edited by K. F. Connor, pp. 92–98, U.S. Dep. of Agric. For. Serv. South. Res. Station, Ashville, N. C.

Hansen, J. E., M. Sato, A. Lacis, R. Ruedy, I. Tegen, and E. Matthews (1998), Climate forcings in the industrial era, *Proc. Natl. Acad. Sci. U. S. A.*, *95*, 12,753–12,758.

Hornbeck, J. W., C. W. Martin, R. S. Pierce, F. H. Bormann, G. E. Likens, and J. S. Eaton (1986), Clearcutting northern hardwoods: Effects on hydrologic and nutrient ion budgets, *For. Sci.*, *32*, 667–686.

Houghton, R. A., J. E. Hobbie, and J. M. Melillo (1983), Changes in the carbon content of terrestrial biota and soils between 1860 and 1980: A net release of CO_2 to the atmosphere, *Ecol. Monogr.*, *53*, 235–262.

Houghton, R. A., et al. (1987), The flux of carbon from terrestrial ecosystems to the atmosphere in 1980 due to changes in land use: Geographic distribution of the global flux, *Tellus, Ser. B*, *39*, 122–139.

Jackson, D. D. (1972), Interpretation of inaccurate, insufficient, and inconsistent data, *Geophys. J. R. Astron. Soc.*, *28*, 97–110.

Johnson, J. E., D. W. Smith, and J. A. Burger (1985), Effects on the forest floor of whole-tree harvesting in an Appalachian oak forest, *Am. Mid. Nat.*, *114*, 51–61.

Johnson, C. E., C. T. Driscoll, T. J. Fahey, T. G. Siccama, and J. W. Hughes (1995), Carbon dynamics following clear-cutting of a northern hardwood forest, in *Carbon Forms and Functions in Forest Soils*, edited by W. W. McFee and J. M. Kelly, pp. 463–488, Soil Sci. Soc. Am., Madison, Wis.

Karl, T. R., J. D. Tarpley, R. G. Quayle, H. F. Diaz, D. A. Robinson, and R. S. Bradley (1989), The recent climate record: What it can and cannot tell us, *Rev. Geophys.*, *27*, 405–430.

Kaufmann, R. K., L. Zhou, R. B. Myneni, C. J. Tucker, D. Slayback, N. V. Shabanov, and J. Pinzon (2003), The effect of vegetation on surface temperature: A statistical analyzis of NDVI and climate data, *Geophys. Res. Lett.*, *30*(22), 2147, doi:10.1029/2003GL018251.

Kraske, C. R. (1992), The influence of papermill sludge application on the biogeochemistry and vegetation of young red pine plantations established

in recent clearcut forest ecosystems, Ph.D. dissertation, Univ. of Maine, Orono.
Lachenbruch, A. H., and B. V. Marshall (1986), Changing climate: Geothermal evidence from permafrost in the Alaskan Arctic, *Science*, *234*, 689–696.
Lanczos, C. (1961), *Linear Differential Operators*, 564 pp., Van Nostrand Reinhold, Hoboken, N. J.
Lane, E. C. (1923), Geotherms of the Lake Superior Copper County, *J. Geol.*, *42*, 113–122.
Lewis, T. J., and K. Wang (1998), Geothermal evidence for deforestation-induced warming: Implications for the climatic impact of land development, *Geophys. Res. Lett.*, *25*, 535–538.
Londo, A. J., M. G. Messina, and S. H. Schoenholtz (1999), Forest harvesting effects on soil temperature, moisture, and respiration in a bottomland hardwood forest, *Soil Sci. Soc. Am. J.*, *63*, 637–644.
Lugo, A. L., and S. Brown (1986), Steady state terrestrial ecosystems and the global carbon cycle, *Vegetatio*, *68*, 83–90.
Lytle, E. D., and C. S. Cronan (1998), Comparative soil CO_2 evolution, litter decay, and root dynamics in clearcut and uncut spruce-fir forest, *For. Ecol. Manage.*, *103*, 121–128.
Mareschal, J. C., and H. Beltrami (1992), Evidence for recent warming from perturbed geothermal gradients: Examples from eastern Canada, *Clim. Dyn.*, *6*, 135–143.
Mattson, K. G., and H. C. Smith (1993), Detrital organic matter and soil CO_2 efflux in forests regenerating from cutting in West Virginia, *Soil Biol. Biochem.*, *25*, 1241–1248.
McGrath, T. (1999), Predicting stand level response to pre-commercial and commercial thinnings, in *Thinning in the Maine Forest: Conference Proceedings, 15–16 November 1999*, edited by R. G. Wagner et al., pp. 13–18, Univ. of Maine, Augusta.
Menke, W. (1989), *Geophysical Data Analysis: Discrete Inverse Theory*, *Int. Geophys. Ser.*, vol. 45, 289 pp., Elsevier, New York.
Oke, T. R. (1987), *Boundary Layer Climates*, 2nd ed., 435 pp., Cambridge Univ. Press, New York.
Pielke, R. A., R. Avissar, M. Raupach, A. J. Dolman, X. Zeng, and A. S. Denning (1998), Interactions between the atmosphere and terrestrial ecosystems: Influence on weather and climate, *Global Change Biol.*, *4*, 461–475.
Plotnikoff, M. R., C. E. Bulmer, and M. G. Schmidt (2002), Soil properties and tree growth on rehabilitated forest landings in the interior cedar hemlock biogeoclimatic zone: British Columbia, *For. Ecol. Manage.*, *170*, 199–215.
Risk, D., L. Kellman, and H. Beltrami (2002a), Carbon dioxide in soil profiles: Production and temperature dependence, *Geophys. Res. Lett.*, *29*(6), 1087, doi:10.1029/2001GL014002.
Risk, D., L. Kellman, and H. Beltrami (2002b), Soil CO_2 production and surface flux at four climate observatories in eastern Canada, *Global Biogeochem. Cycles*, *16*(4), 1122, doi:10.1029/2001GB001831.
Schneider, S. H. (1990), *Global Warming: Are We Entering the Greenhouse Century?*, 343 pp., Vintage Books, San Francisco, Calif.
Schneider, S. H. (1995), Introduction, in *Climate System Modeling*, edited by K. E. Trenberth, pp. 689–705, Cambridge Univ. Press, New York.
Shukla, J., C. Nobre, and P. Sellers (1990), Amazon deforestation and climate change, *Science*, *247*, 1322–1325.
Vasseur, G., P. Bernard, J. Van De Meulebrouck, Y. Kast, and J. Jolivet (1983), Holocene paleotemperatures deduced from geothermal measurements, *Palaeogeogr. Palaeoclimatol. Palaeoecol.*, *43*, 237–259.
Yanai, R. D. (1992), The phosphorus budget of a 70-year-old northern hardwood forest, *Biogeochemistry*, *17*, 1–22.
Yanai, R. D., S. C. William, and C. L. Goodale (2003), Soil carbon dynamics after forest harvest: An ecosystem paradigm reconsidered, *Ecosystems*, *6*, 197–212.
Yoshikawa, K., W. R. Bolton, V. E. Romanovsky, M. Fukuda, and L. D. Hinzman (2003), Impacts of wildfire on the permafrost in the boreal forests of interior Alaska, *J. Geophys. Res.*, *108*(D1), 8148, doi:10.1029/2001JD000438.
Zeng, N., and J. D. Neelin (1999), A land-atmosphere interaction theory for the tropical deforestation problem, *J. Clim.*, *12*, 857–872.
Zhang, H., A. Handerson-Sellers, and K. McGuffie (1996), Impacts of tropical deforestation. part I: Process analysis of local climatic change, *J. Clim.*, *9*, 1497–1517.

H. Beltrami and D. Nitoiu, Environmental Sciences Research Centre, St. Francis Xavier University, P.O. Box 5000, Antigonish, Nova Scotia, Canada B2G 2W5. (hugo@stfx.ca; dnitoiu@stfx.ca)